Close-to-Ground Single Antenna GNSS-R

Corentin Lubeigt, Francois Vincent, Lorenzo Ortega, Jordi Vilà-Valls, Laurent Lestarquit, Eric Chaumette

HAL Id: hal-03758599

https://hal.science/hal-03758599

Submitted on 23 Aug 2022

Close-to-Ground Single Antenna GNSS-R

Corentin Lubeigt[1,2], François Vincent[2], Lorenzo Ortega[3], Jordi Vilà-Valls[2], Laurent Lestarquit[4], and Eric Chaumette[2]

[1] *TéSA Laboratory*
31500 Toulouse, France
Email: corentin.lubeigt@tesa.prd.fr
[2] *ISAE-SUPAERO*
31400 Toulouse, France
Emails: {francois.vincent, jordi.vila-valls, eric.chaumette}@isae-supaero.fr
[3] *IPSA*
31000 Toulouse, France
Email: lorenzo.ortega@ipsa.fr
[4] *CNES*
31400, Toulouse, France
Email: laurent.lestarquit@cnes.fr

Abstract

For more than three decades, Global Navigation Satellite System (GNSS) signals have been seen as signals of opportunity as in GNSS Reflectometry (GNSS-R). The study of the reflections from the ground of such signals can indeed lead to many features regarding the reflecting surface and the receiver's height. Due to the nature of the GNSS signal, that is, due to its wavelength, the distortion of the reflected signal may vary significantly depending on the reflecting surface and on the dynamic and height of the receiver. The latter does range from low earth orbit down to ground-based platforms. In this last case, the vicinity to the ground induces important interference between the direct and the reflected path which makes it difficult to process directly in order to obtain altimetry product. In this study, the feasibility of ground-based single antenna GNSS-R altimetry is studied and solutions are presented depending on the satellite elevation angle. To do so, maximum-likelihood-based algorithms - namely the CLEAN-RELAX Estimator and the Approximate Maximum Likelihood Estimator - are presented and applied to a set of scenarios.

INTRODUCTION

For almost thirty years, Global Navigation Satellite System (GNSS) signals have been considered not only as a mean to obtain time, position and velocity on Earth but also as signals of opportunity for scores of applications. For instance GNSS Reflectometry (GNSS-R) focuses on the reflection of these signals upon the Earth to extract features such as soil moisture, sea state, sea surface height, etc.

GNSS-R can be performed from spaceborne receivers such as TDS-1, CYGNSS or the coming HydroGNSS missions where the reflected signal is strongly distorted due to the large reflecting surface, the atmosphere crossed twice and the important velocity variations of both the GNSS satellite and the receiver's platform. It can also be performed from an airborne platform such as Software PARIS Interferometric Receiver (SPIR) or Microwave Interferometric Reflectometer (MIR). For spaceborne and airborne scenarios, the path separation between the line-of-sight (LOS) signal and its reflection is large enough to be processed separately. Moreover, the polarity of the reflected signal being inverted due to the reflection, the signals is always collected with two antennas: one upward with a right-hand circular polarization (RHCP) and the other, down-looking with a left-hand circular polarization (LHCP). In these two cases, the reflected path is usually correlated with either a clean replica, as in conventional GNSS-R (cGNSS-R) or the LOS signal itself as in interferometric GNSS-R (iGNSS-R).

Finally, it can be performed from ground-based stations from where the path separation is so short that a potential interference between the LOS signal and its reflection often happens. In this scenario, cGNSS-R and iGNSS-R techniques may not work due to the reflected path interfering with the LOS. A common approach to actually study this interference, so-called GNSS Interferometric Reflectometry (GNSS-IR), estimates the fringes of signal-to-noise ratio (SNR) due to the successive constructive and destructive recombinations of the LOS and the reflected path as the satellite elevation varies.

Such a technique uses a single antenna and exploits the small portion of the reflected path that impinges it. The oscillation depending on the elevation satellite, it requires several minutes to obtain an estimate [1]. It is however less common to process the combined signals in order to extract the path separation from the estimated delays as it is done in cGNSS-R.

In this contribution, the feasibility of ground-based, single antenna altimetry with GNSS-R is studied. To do so, a first section will present the signal model considered along with different parameters to be estimated, then two Maximum Likelihood-based algorithms are presented: the first one, the Approximate Maximum Likelihood Estimator (AMLE) [2] which exploits the fact that when the path separation is small enough, a second order Taylor approximation of the likelihood criterion can simplify the estimation formulation. The second estimator, the CLEAN-RELAX Estimator (CRE) or Multipath Estimating Delay Lock Loop (MEDLL) [3] which is a suboptimal version of the dual source Maximum Likelihood Estimator (2S-MLE). Once these algorihtms presented, they are applied to two scenarios through Monte Carlo simulations and a discussion is drawn from the obtained results.

SIGNAL MODEL

In this study, a receiver with a single antenna able to collect both a direct signal (indexed 0) and its reflection (indexed 1) is considered. The receiver is assumed close to the ground and the reflection, caused by a smooth surface such as a lake is assumed specular.

The transmitter T is emitting a band-limited signal $s(t)$ with bandwidth B, over a carrier frequency f_c. This signal can be expressed as follows:

$$s(t) = \sum_{n=N_1'}^{N_2'} s\left(\frac{n}{B}\right) \text{sinc}\left(\pi B\left(t - \frac{n}{B}\right)\right) \leftrightharpoons S(f) = \frac{1}{B}\sum_{n=N_1'}^{N_2'} s\left(\frac{n}{B}\right) e^{-j2\pi n \frac{f}{B}}, \quad -\frac{B}{2} \leq f \leq \frac{B}{2}, \tag{1}$$

where $\text{sinc}(\cdot)$ is the sine cardinal function, f the frequency, $N_1', N_2' \in \mathbb{Z}$, $N_1' < N_2'$ and $\leftrightharpoons$ refers to the time-frequency pair.

The received signal at the antenna input can then be expressed as a sum of two delayed and attenuated copies of the same signal:

$$x_R(t) \approx x(t)e^{j\omega_c t}, \tag{2}$$

$$x(t) \triangleq d(t; \tau_0, b_0, \rho_0, \phi_0) + d(t; \tau_0 + \Delta\tau, b_1, \rho_1, \phi_1) + w(t), \tag{3}$$

$$d(t; \tau, \rho, \phi) = \rho e^{j\phi} s\left(t - \tau\right) e^{-j2\pi f_c bt}, \tag{4}$$

where $w(t)$ is a zero-mean white complex Gaussian noise, $\omega_c = 2\pi f_c$, τ_0 is the time delay of the direct signal, $\Delta\tau$ is the excess delay of the reflected signal relatively to the τ_0 and for $i \in \{0, 1\}$ b_i is the Doppler stretch, ρ_i and ϕ_i, the amplitude (strictly positive) and the phase of the complex coefficient induced by propagation characteristics (fading, scintillation, etc).

Now, considering the acquisition of $N = N_2 - N_1$ ($N_1 \ll N_1', N_2 \gg N_2'$) samples at a sampling rate $T_s = 1/F_s$ where F_s is taken equal to the RF front-end bandwidth, the baseband output of the Hilbert's filter, assuming a perfect Doppler compensation as it is discussed in the following section, results in the following discrete signal model that can be identified with a dual source Conditional Signal Model (CSM) as in [4]:

$$\mathbf{x} = \mathbf{A}(\tau_0, \Delta\tau)\boldsymbol{\alpha} + \mathbf{w}, \quad \mathbf{w} \sim \mathcal{CN}(0, \sigma_n^2 \mathbf{I}_N), \tag{5}$$

with, for $n \in [N_1, N_2]$,

$$\mathbf{x}^T = (\dots, x(nT_s), \dots), \tag{6}$$

$$\mathbf{A}(\tau_0, \Delta\tau) = [\mathbf{s}(\tau_0), \mathbf{s}(\tau_0 + \Delta\tau)], \tag{7}$$

$$\mathbf{s}(\tau)^T = (\dots, s(nT_s - \tau) \dots), \tag{8}$$

$$\boldsymbol{\alpha}^T = \left(\rho_0 e^{j\phi_0}, \rho_1 e^{j\phi_1}\right), \tag{9}$$

$$\mathbf{w}^T = (\dots, w(nT_s), \dots). \tag{10}$$

Doppler Frequency Consideration

In the model (5), the Doppler frequencies of the signal and its reflection are assumed equal and perfectly compensated. In the case of a static ground-based scenario, it can be shown that the Doppler frequency difference between the direct

signal and its reflection is only due to the receiver height and the elevation of the satellite: indeed, for very low altitude scenarios, the phase difference between the direct and the reflected path can be expressed as follows [5]:

$$\Delta \phi = \phi_1 - \phi_0 = \frac{2\omega_c h}{c} \sin(e). \tag{11}$$

Then, as the satellite elevation e varies, the relative phase varies and the first derivative corresponds to the relative Doppler frequency:

$$\Delta F_d = (b_1 - b_0)f_c = \frac{2f_c h}{c} \cos(e)\frac{\mathrm{d}e}{\mathrm{d}t}. \tag{12}$$

Expression (12) is often used to do altimetry based on the SNR observations [1, 6] in GNSS-IR. A worst-case numerical application yields, for GPS L1 satellites with elevation rate $\mathrm{d}e/\mathrm{d}t = 0.14$ mrad/s, $e = 0$ rad, $f_c = 1.545$ GHz and a receiver at altitude $h = 75$ m: $\Delta F_d \approx 0.12$ Hz. Such a small difference will not be observable for coherent integration time considered in this study.

ALGORITHMS

Given the dual source CSM (5), it is well known that the corresponding 2S-MLE of $\boldsymbol{\xi} \triangleq [\tau_0, \Delta\tau, \rho_0, \phi_0, \rho_1, \phi_1]^T$ is given by [7, 8]:

$$\left(\widehat{\tau_0}, \widehat{\Delta\tau}\right) = \arg \max_{\tau_0, \Delta\tau} \|\mathbf{P_A x}\|^2 \tag{13}$$

and, for $(\tau_0, \Delta\tau) = \left(\widehat{\tau_0}, \widehat{\Delta\tau}\right)$ and $i \in \{0, 1\}$,

$$\widehat{\rho}_i = \left| \left[\left(\mathbf{A}^H\mathbf{A}\right)^{-1} \mathbf{A}^H\mathbf{x} \right]_i \right|, \tag{14}$$

$$\widehat{\phi}_i = \arg\left\{ \left[\left(\mathbf{A}^H\mathbf{A}\right)^{-1} \mathbf{A}^H\mathbf{x} \right]_i \right\}, \tag{15}$$

$$\widehat{\sigma_n^2} = \frac{1}{N} \left\|\mathbf{P_A^\perp x}\right\|^2 \tag{16}$$

where $\mathbf{P_A} = \mathbf{A}\left(\mathbf{A}^H\mathbf{A}\right)^{-1}\mathbf{A}^H$ is the projection onto the subspace spanned by the columns of $\mathbf{A}$ (signal subspace) and $\mathbf{P_A^\perp} = \mathbf{I} - \mathbf{P_A}$ is the projection onto the noise subspace.

The following sections present algorithms based on the 2S-MLE, first by assuming the path separation $\Delta\tau$ to be very small and by performing a Taylor expansion of the likelihood criterion (13). Then by iteratively finding the maximum with regard to one source and fixing the other and vice versa.

Approximate Maximum Likelihood Estimator

In this study, the AMLE presented in [2] is adapted to the problem of close-in-time sources instead of close-in-frequency sources. Based on the signal model described in (5). The likelihood criterion, noted $L(\tau_0, \Delta\tau)$, to be maximized is defined by (13). It can be written as follows:

$$L(\tau_0, \Delta\tau) \triangleq \|\mathbf{P_A x}\|^2 = \mathbf{x}^H\mathbf{P_A x} = \left(\mathbf{A}^H\mathbf{x}\right)^H \left(\mathbf{A}^H\mathbf{A}\right)^{-1} \mathbf{A}^H\mathbf{x} \tag{17}$$

where the inverse matrix can be explicitly written with regard to (w.r.t.) the path separation $\Delta\tau$:

$$\left(\mathbf{A}^H\mathbf{A}\right)^{-1} \propto \frac{1}{1 - |c(\Delta\tau)|^2} \begin{bmatrix} 1 & -c(\Delta\tau) \\ -c(\Delta\tau)^* & 1 \end{bmatrix} \tag{18}$$

where $c(\Delta\tau) \propto \mathbf{a}_0^H\mathbf{a}_1$ is the normalized auto-correlation of the signal expressed in $\Delta\tau$. A key point for the coming development is that this auto-correlation depends only on $\Delta\tau$.

From the signal discrete signal model (5), if the number of elements $N_2 - N_1$ is very large, the auto-correlation function $c(\Delta\tau)$ can be written as an integral:

$$c(\Delta\tau) \propto \mathbf{a}_0^H\mathbf{a}_1 = F_s \int_{\mathbb{R}} s(t - \tau_0)^* s(t - \tau_0 - \Delta\tau)\mathrm{d}t = F_s \int_{\mathbb{R}} s(u)^* s(u - \Delta\tau)\mathrm{d}u. \tag{19}$$

Then, using the Fourier transform properties over the hermitian product and the sum definition of the Fourier transform recalled in (1):

$$c(\Delta\tau) = F_s \int_{-F_s/2}^{F_s/2} \left(\frac{1}{F_s} \sum_{n=N_1}^{N_2} s(nT_s)e^{-j2\pi fnT_s} \right)^* \left(\frac{1}{F_s} \sum_{n=N_1}^{N_2} s(nT_s)e^{-j2\pi fnT_s} \right) e^{-j2\pi f\Delta\tau} \mathrm{d}f \tag{20}$$

$$= \mathbf{s}^H \left(\int_{-1/2}^{1/2} \boldsymbol{\nu}(f)\boldsymbol{\nu}(f)^H e^{-j2\pi fF_s\Delta\tau} \mathrm{d}f \right) \mathbf{s} = \mathbf{s}^H \mathbf{D}(\Delta\tau)\mathbf{s} \tag{21}$$

where

$$\mathbf{s} = (\ldots,\, s(nT_s),\, \ldots)^T_{N_1 \le n \le N_2}\,, \tag{22}$$

$$\boldsymbol{\nu}(f) = (\ldots,\, e^{j2\pi fn},\, \ldots)^T_{N_1 \le n \le N_2}\,, \tag{23}$$

$$\mathbf{D}(\Delta\tau) = \int_{-1/2}^{1/2} \boldsymbol{\nu}(f)\boldsymbol{\nu}(f)^H e^{-j2\pi fF_s\Delta\tau}\mathrm{d}f. \tag{24}$$

From relations (21) and (24) and the Taylor expansions of $c(\Delta\tau)$ and $\mathbf{D}(\Delta\tau)$, it is then possible to directly apply the formula [2, (11)] and obtain a second order Taylor expansion of the likelihood criterion:

$$L(\tau_0, \Delta\tau) \approx L^{\text{Taylor}}(\tau_0, \Delta\tau) = L_0(\tau_0) + L_1(\tau_0)\Delta\tau + L_2(\tau_0)\Delta\tau^2 \tag{25}$$

where the coefficients $L_k(\tau_0)$ for $k \in \{0, 2\}$ are expressed as the convolution of the consecutive derivatives of the auto-correlation function.

Then, by differentiating (25) with respect to $\Delta\tau$ and zeroing this first derivative, a closed-form expression for all τ_0 of the relative path maximizing the likelihood criterion can be obtained:

$$\Delta\tau^{\text{AMLE}}(\tau_0) = -\frac{L_1(\tau_0)}{2L_2(\tau_0)} \tag{26}$$

and, injecting (26) into (25), maximizing the likelihood criterion reduces to a one dimensional search:

$$\max_{\tau_0, \Delta\tau} L(\tau_0, \Delta\tau) \approx \max_{\tau_0} L^{\text{Taylor}}\left(\tau_0, \Delta\tau^{\text{AMLE}}(\tau_0)\right) \tag{27}$$

From the solution of (27), it is therefore possible to recover the estimated path separation by using relation (26) expressed w.r.t. $\widehat{\tau_0}$.

An important note regarding this approach is that since a Taylor approximation of the auto-correlation function is at the origin of all the calculation, the resulting algorithm cannot be expected to work properly when the path separation is too far from zero. Consequently, the AMLE will be a relevant choice of algorithm only in the case of very short path separation when, in the case of GNSS-R, the transmitting satellite's elevation is small enough or in the case of very close-to-ground receiver platform.

CLEAN-RELAX Estimator

The CLEAN-RELAX Estimator (CRE), also known as MEDLL is a suboptimal version of the 2S-MLE. It consists of iteratively estimating a single source and its parameter: that is, for the ith iteration, finding $(\tau_0^{(i)}, \rho_0^{(i)}, \phi_0^{(i)})$ and removing this estimation from the received signal in order to estimate a second signal and its parameters $(\tau_1^{(i)}, \rho_1^{(i)}, \phi_1^{(i)})$ from the residue. These iterations are done until the residual error is stabilized. The performance of this estimator were first studied in [9] and more recently in [10]. Fig. 1 represents the multipath error envelope [11] (MPEE) for this estimator, assuming a given RF front-end bandwidth equal to 4 MHz and an amplitude ratio of 0.5 between the reflected path and the direct one. In Fig. 1, one can note that under a certain value of path separation (in this case, about 135m) and depending on the relative phase between the direct and the reflected path, the CRE can be biased, that is, the reflected path induces an error on the estimation of the direct signal's delay. Above this value, the CRE is unbiased and is able to separate both sources.

As a consequence, the CRE may not do very well when the path separation is too small but if it gets larger, the transmitting satellite being supposedly higher in the sky, this algorithm seems an adequate choice to efficiently estimate the resulting path separation.
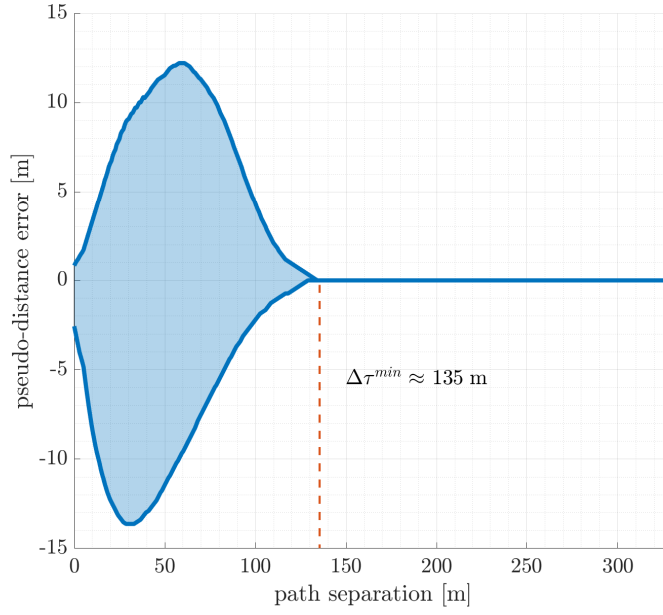
Fig. 1. MPEE for the CRE, RF front-end bandwidth is set to 4 MHz.

RESULTS AND DISCUSSIONS

Simulation Set-up

In order to illustrate the presented algorithms, a set of Monte Carlo simulations have been performed and the root mean square error (RMSE) of both the AMLE and the CRE $\Delta\tau$ estimation has been calculated and compared to the corresponding Cramér-Rao Bounds (CRB). Two scenarios, illustrated by Fig. 2, are considered:

- Scenario 1: the transmitting satellite has a low elevation angle e_1, the resulting path separation is very small and the CRE cannot perform properly, in this case, the AMLE's assumption of very small path separation is valid.

- Scenario 2: the transmitting satellite is now very high in the sky (elevation angle e_2), the path separation is too large for the AMLE to work but the CRE is now able to separate the two signals.
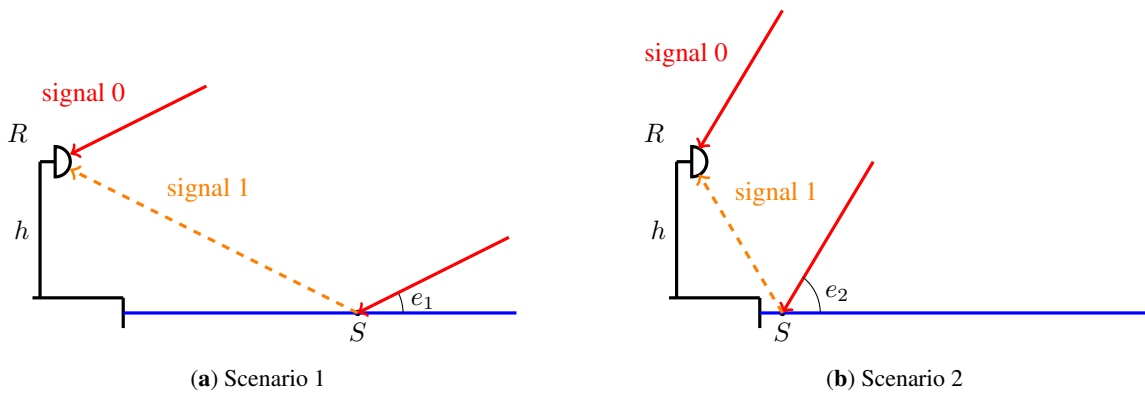

(**a**) Scenario 1 (**b**) Scenario 2

Fig. 2. Scenarios considered in the simulations: Scenario 1 (**a**): low elevation angle e_1 and small path separation adapted to AMLE. Scenario 2 (**b**): high elevation angle e_2 and large path separation adapted to CRE.

For each scenario, the receiver is supposed to have a RF front-end bandwidth set to 4 MHz and the signal is sampled at the Nyquist frequency. The signal consists of a GPS L1 C/A and its reflection, coherently integrated during $T_I = 4$ms.

The reflected path has an amplitude set to half the amplitude of the direct signal $\rho_1 = \rho_0/2$ and the relative phase is set to two arbitrary values $\Delta\phi = \pi/3$ and $\Delta\phi = \pi/2$. Each point presented in the following figures was obtained with 2000 Monte Carlo runs. The RMSE is computed with regard to the SNR at the output of the matched filter, defined as follows:

$$\text{SNR}_{\text{out}} = \frac{\rho_0^2 \mathbf{s}^H \mathbf{s}}{\sigma_n^2} \tag{28}$$

If one considers a receiver set at $h = 75$m above the targeted reflecting surface, from the well-known equation that links the height with the path separation $\Delta\tau$ and the elevation angle of the satellite e:

$$\Delta\tau = 2\frac{h}{c}\sin(e), \tag{29}$$

it is possible to fix the satellite elevation depending on the scenarios. Table 1 summarizes the chosen elevation angle values and the corresponding path separations:

Table 1: Recap of the elevation angles and corresponding path separation for the considered scenarios

	elev. angle e [°]	path sep. $\Delta\tau$ [C/A chips]	path sep. $\Delta\tau$ [m]
Scenario 1	4.5	0.04	11.7
Scenario 2	77	0.5	146.5

Cramér-Rao Bounds

Considering the signal model and starting from the joint delay-Doppler estimation problem presented in [4] for the estimation of $\boldsymbol{\epsilon} = [\sigma_n^2, \tau_0, b_0, \rho_0, \phi_0, \tau_1, b_1, \rho_1, \phi_1]^T$, where b_0 and b_1 are the Doppler terms of the direct and reflected signal, respectively, that are assumed equal and compensated in this study, it is straightforward to obtain an expression of the Fisher Information Matrix (FIM) for the estimation of $\boldsymbol{\xi} = [\sigma_n^2, \tau_0, \Delta\tau, \rho_0, \phi_0, \rho_1, \phi_1]^T$:

$$\mathbf{FIM}_{\boldsymbol{\xi}|\boldsymbol{\xi}} = \left(\frac{\partial\boldsymbol{\epsilon}}{\partial\boldsymbol{\xi}^T}\right)^T \mathbf{FIM}_{\boldsymbol{\epsilon}|\boldsymbol{\epsilon}} \frac{\partial\boldsymbol{\epsilon}}{\partial\boldsymbol{\xi}^T} \tag{30}$$

where $\partial\boldsymbol{\epsilon}/\partial\boldsymbol{\xi}^T$ is the jacobian of the application for which the image of $\boldsymbol{\epsilon}$ is $\boldsymbol{\xi}$. The CRB for the estimation of $\boldsymbol{\xi}$ is the inverse of the resulting FIM.

Scenario 1: Low Elevation Angle with AMLE

In Fig. 3, the RMSE for the estimation of the path separation $\Delta\tau$ using the AMLE is displayed along with the corresponding CRB. First, one can notice that the convergence of the AMLE, observable when the RMSE curves are parallel to the CRB ones, is obtained for very large output SNR values which was expected since the sources are very close, the algorithm then requires a very good signal quality to separate the two delays. Another observation is that there remains a small bias due to the Taylor approximation: indeed in the convergence region (above 40dB), there is a constant offset between the RMSE and the CRB. By running the AMLE with a noise-free signal, it is possible to evaluate the bias of the algorithm for these two specific relative phases: for both values of $\Delta\phi$, the value of the bias is found to be close to 0.45m.

Regarding this scenario, a final note must be added concerning the order of magnitude of the RMSE. For SNR=40dB, the expected standard deviation of the estimated path separation cannot better 10m, if one wants to obtain accurate measure, of the order of 1m or less, they would need to integrate for a longer time (a few seconds) to obtain the required SNR.

Scenario 2: Large Elevation Angle with CRE

In Fig. 4, the RMSE in the case of a high elevation angle and using the CRE is displayed with the corresponding CRB. In this figure, the RMSE and the CRB for $\Delta\phi = \pi/3$ and $\Delta\phi = \pi/2$ are very close. It is clear that for such a path separation, the algorithm RMSE asymptotically reaches the CRB, this convergence is obtained when the SNR is larger than 24dB. This result is coherent with the CRE MPEE presented in Fig. 1.

The sources being more separated in this scenario, the SNR required to efficiently estimate the path separation is significantly smaller than the one for the first scenario. In this case, the RMSE reaches the CRB at a SNR of about 25dB. For this noise level, the CRB is of about 10m. Again, integrating the signal for a longer time would allow to obtain better precision.
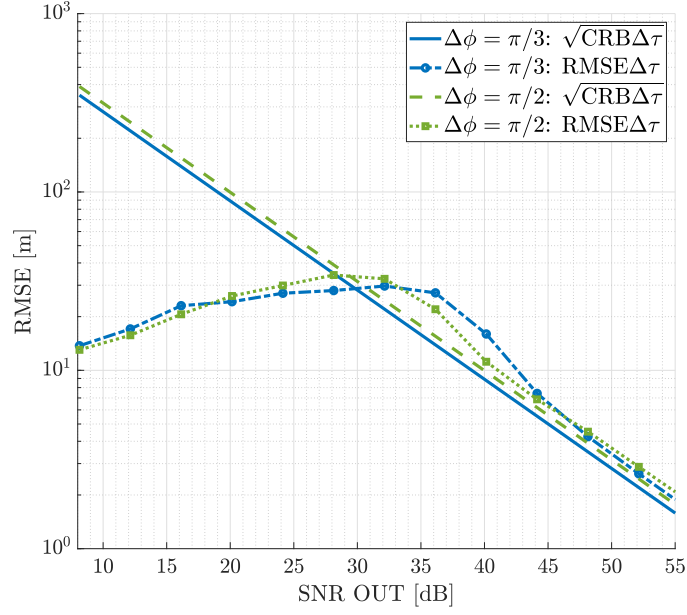
Fig. 3. Approximate Maximum Likelihood estimator RMSE for the estimation of the path separation $\Delta\tau$ in the low elevation angle scenario (scenario 1) for two different relative phases $\Delta\phi = \pi/3$ and $\Delta\phi = \pi/2$.
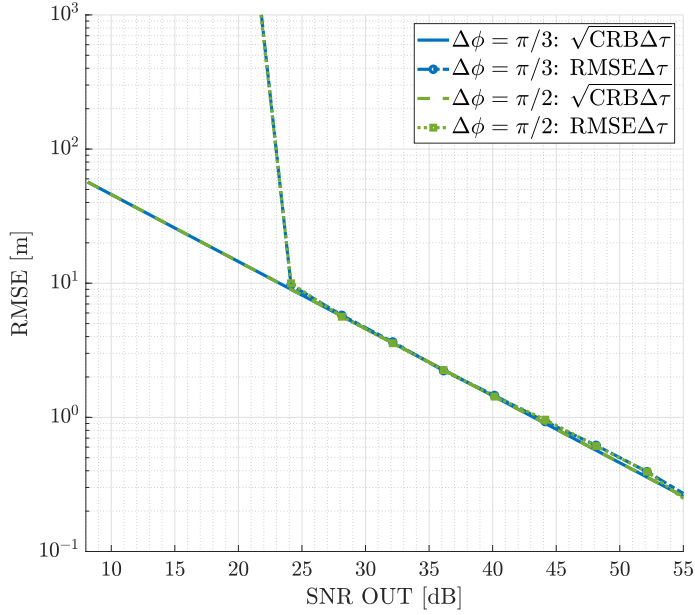

Fig. 4. CLEAN-RELAX estimator RMSE for the estimation of the path separation $\Delta\tau$ in the low elevation angle scenario (scenario 1) for two different relative phases $\Delta\phi = \pi/3$ and $\Delta\phi = \pi/2$.

CONCLUSION

In this paper, the feasibility of close-to-ground, single antenna, GNSS-R altimetry was studied in a different way than the common GNSS-IR approach. Along with the already known CLEAN-RELAX Estimator, or MEDLL, a direct implementation of the Approximate Maximum Likelihood estimator, which is based on a second order Taylor approximation of the likelihood criterion was presented. From Monte Carlo simulations, it was shown that for large enough path separation,

the CRE proves to be an efficient solution for the estimation of the path separation. When the path separation gets very small, however, the CRE does not perform well anymore and the AMLE happens to be a good candidate for large SNR.

REFERENCES

[1] M. A. Ribot, J.-C. Kucwaj, C. Botteron, S. Reboul, G. Stienne, J. Leclère, J.-B. Choquel, P.-A. Farine, and M. Benjelloun, "Normalized GNSS Interference Pattern Technique for Altimetry," *Sensors*, vol. 14, no. 6, pp. 10 234–10 257, 2014. [Online]. Available: https://www.mdpi.com/1424-8220/14/6/10234

[2] F. Vincent, O. Besson, and E. Chaumette, "Approximate Maximum Likelihood Estimation of Two Closely Spaced Sources," *Signal Processing*, vol. 97, pp. 83–90, 2014. [Online]. Available: http://www.sciencedirect.com/science/article/pii/S0165168413004088

[3] R. D. Van Nee, "The Multipath Estimating Delay Lock Loop," in *IEEE Second International Symposium on Spread Spectrum Techniques and Applications*, 1992, pp. 39–42.

[4] C. Lubeigt, L. Ortega, J. Vilà-Valls, L. Lestarquit, and E. Chaumette, "Joint Delay-Doppler Estimation Performance in a Dual Source Context," *Remote Sensing*, vol. 12, no. 23, 2020. [Online]. Available: https://www.mdpi.com/2072-4292/12/23/3894

[5] Y. Georgiadou and A. Kleusberg, "On Carrier Signal Multipath Effects in Relative GPS Positioning," *Manuscripta Geodaetica*, vol. 13, no. 3, pp. 172–179, 1988.

[6] K. M. Larson, E. E. Small, E. D. Gutmann, A. L. Bilich, J. J. Braun, and V. U. Zavorotny, "Use of GPS Receivers as a Soil Moisture Network for Water Cycle Studies," *Geophysical Research Letters*, vol. 35, no. 24, 2008.

[7] P. Stoica and A. Nehorai, "MUSIC, Maximum Likelihood, and Cramér-Rao Bound," *IEEE Transactions on Acoustics, Speech, and Signal Processing*, vol. 37, no. 5, pp. 720–741, 1989.

[8] B. Ottersten, M. Viberg, P. Stoica, and A. Nehorai, "Exact and Large Sample Maximum Likelihood Techniques for Parameter Estimation and Detection in Array Processing," in *Radar Array Processing*, S. Haykin, J. Litva, and T. J. Shepherd, Eds. Heidelberg: Springer-Verlag, 1993, ch. 4, pp. 99–151.

[9] B. R. Townsend, P. C. Fenton, K. J. Van Dierendonck, and R. D. J. Van Nee, "Performance Evaluation of the Multipath Estimating Delay Lock Loop," *Navigation*, vol. 42, no. 3, pp. 502–514, 1995. [Online]. Available: https://onlinelibrary.wiley.com/doi/abs/10.1002/j.2161-4296.1995.tb01903.x

[10] C. Lubeigt, L. Ortega, J. Vilà-Valls, L. Lestarquit, and E. Chaumette, "On the Impact and Mitigation of Signal Crosstalk in Ground-Based and Low Altitude Airborne GNSS-R," *Remote Sensing*, vol. 13, no. 6, p. 1085, 2021.

[11] E. Kaplan and C. Hegarty, *Understanding GPS/GNSS: Principle and Applications*, 3rd ed. Artech House, 2017.